QUADRATIC AUXILIARY VARIABLE RUNGE-KUTTA METHODS FOR THE CAMASSA-HOLM EQUATION

YUEZHENG GONG *, QI HONG †, CHUNWU WANG ‡, AND YUSHUN WANG §

Abstract. In this paper, we propose a novel class of Runge-Kutta methods for the Camassa-Holm equation, which is named quadratic auxiliary variable Runge-Kutta (QAVRK) methods. We first introduce an auxiliary variable that satisfies a quadratic equation and rewrite the original energy into a quadratic functional. With the aid of the energy variational principle, the original system is then reformulated into an equivalent form with two strong quadratic invariants, where one is induced by the quadratic auxiliary variable and the other is the modified energy. Starting from the equivalent model, we employ RK methods satisfying the symplectic condition for time discretization, which naturally conserve all strong quadratic invariants of the new system. The resulting methods are shown to inherit the relationship between the auxiliary variable and the original one, and thus can be simplified by eliminating the auxiliary variable, which leads to a new class of QAVRK schemes. Furthermore, the QAVRK methods are proved rigorously to preserve the original energy conservation law. Numerical examples are presented to confirm the expected order of accuracy, conservative property and efficiency of the proposed schemes. This numerical strategy makes it possible to directly apply the symplectic RK methods to develop energy-preserving algorithms for general conservation systems with any polynomial energy.

Key words. Camassa-Holm equation, Quadratic auxiliary variable, High-order schemes, Energy-preserving methods.

AMS subject classifications. 65M06, 65M70

1. Introduction.

In this paper, we consider the Camassa-Holm (CH) equation

$$u_t - u_{xxt} + 3uu_x - 2u_xu_{xx} - uu_{xxx} = 0, \quad (x,t) \in [a,b] \times (0,T], \tag{1.1}$$

with periodic boundary condition

$$u(a,t) = u(b,t), \quad t \in [0,T], \tag{1.2}$$

and initial condition

$$u(x,0) = u_0(x), \quad x \in [a,b], \tag{1.3}$$

where u is the fluid velocity in the x direction (or equivalently the height of the fluid's free surface above a flat bottom). The CH equation is a model for the unidirectional propagation of shallow water waves [8] as well as a model for nonlinear waves in cylindrical hyperelastic rods [16]. It has a bi-Hamiltonian structure with an infinite number of conserved functionals [19, 20]. In particular, the CH equation possesses the following three conserved quantities

$$\mathcal{I} = \int_a^b u\mathrm{d}x, \quad \mathcal{M} = \frac{1}{2}\int_a^b (u^2 + u_x^2)\mathrm{d}x, \quad \mathcal{H} = \frac{1}{2}\int_a^b (u^3 + uu_x^2)\mathrm{d}x, \tag{1.4}$$

*Department of Mathematics, Nanjing University of Aeronautics and Astronautics, Nanjing 211106, China; Key Laboratory of Mathematical Modelling and High Performance Computing of Air Vehicles (NUAA), MIIT, Nanjing 211106, China; Jiangsu Key Laboratory for Numerical Simulation of Large Scale Complex Systems, Nanjing 210023, China; Email: gongyuezheng@nuaa.edu.cn

†Department of Mathematics, Nanjing University of Aeronautics and Astronautics, Nanjing 211106, China; Key Laboratory of Mathematical Modelling and High Performance Computing of Air Vehicles (NUAA), MIIT, Nanjing 211106, China; Jiangsu Key Laboratory for Numerical Simulation of Large Scale Complex Systems, Nanjing 210023, China; Email: qhong@nuaa.edu.cn

‡Department of Mathematics, Nanjing University of Aeronautics and Astronautics, Nanjing 211106, China; Key Laboratory of Mathematical Modelling and High Performance Computing of Air Vehicles (NUAA), MIIT, Nanjing 211106, China; Email: wangcw@nuaa.edu.cn

§Corresponding author. Jiangsu Key Laboratory for Numerical Simulation of Large Scale Complex Systems, School of Mathematical Sciences, Nanjing Normal University, Nanjing 210023, China; Email: wangyushun@njnu.edu.cn

where $\mathcal{I}$, $\mathcal{M}$ and $\mathcal{H}$ correspond to mass, momentum and energy of the original problem, respectively.

Because of the rich mathematical structure and interesting properties of CH equation [8,13,19,20,37], it is very important to develop geometric numerical integrators or structure-preserving algorithms for solving the CH equation accurately. In the early days, some spatial structure-preserving algorithms were proposed for the CH equation, including finite difference method [9,30], Fourier spectral or pseudo-spectral method [35,36] and local discontinuous Galerkin method [47], etc. Some adaptive spatial approximations were presented to capture the peakon efficiently [2, 18, 47]. There have also been developed more fully discrete structure-preserving algorithms, such as symplectic or multi-symplectic integrators [6, 11, 44, 50], momentum-preserving methods [12, 39, 41] and energy-preserving algorithms [12, 23, 40]. Most existing conservative schemes are based on discrete variational derivative methods [15, 21], which are often fully implicit. Recently, Hong et al. developed two linear-implicit momentum-conserving schemes, which could preserve the original momentum exactly [31]. According to the polarised discrete gradient methods and the Kahan's method, Eidnes et al. constructed two linearly implicit energy-preserving schemes for the CH equation [17]. Jiang et al. applied the energy quadratization approach [43, 48] to obtain two linear energy-preserving schemes [32,33]. At each time step, the linearly implicit methods only require to solve a linear system, which leads to considerably lower costs than the implicit ones. However, these linear-implicit energy-preserving methods only maintain a modified energy, which is not equal to the original one. In this paper, we will focus on developing numerical methods for preserving the original energy.

Most of the existing structure-preserving algorithms are only up to second order in time, which can not usually provide long time accurate solutions with a given large time step. In recent years, there has been an increasing interest in developing high-order invariant-preserving numerical methods for general conservative systems. It is well known that any Runge-Kutta (RK) method preserves all linear invariants, while only those that satisfy the symplectic condition conserve all quadratic first integrals [14]. However, no RK method can recover arbitrary polynomial invariants of degree greater than two [7]. Over the past decade, many high-order energy-preserving schemes have been developed specifically for conservative systems with gradient structure, including high-order averaged vector field (AVF) methods [38, 42, 46], Hamiltonian Boundary Value Methods (HBVMs) [3–5], energy-preserving variant of collocation methods [10, 28] and time finite element methods [45]. It should be noted that all of these high-order conservative methods involve integrals, which often need to be replaced by high-precision numerical integration formulas for practicality. Therefore, they are able to conserve polynomial invariants exactly, whereas for non-polynomial cases, they do preserve numerically. Recently, based on the energy quadratization techniques [43, 48], some high-order structure-preserving algorithms have been developed for various models, including dissipative systems [1,26,27] and conservative systems [33,34,49]. However, different from existing structure-preserving algorithms, these numerical strategies only maintain a modified quadratic energy, which is not the essential property of the original model. The aim of this paper is to present a new numerical strategy to develop high-order energy-preserving algorithms that conserve the original energy exactly.

In this paper, we propose a new class of quadratic auxiliary variable Runge-Kutta (QAVRK) methods for the CH equation. We first rewrite the original energy into an equivalent quadratic form by introducing a quadratic auxiliary variable (QAV), which satisfies a quadratic function of the original one. Based on the energy variational principle, the CH model is reformulated into an equivalent system with two strong quadratic invariants, one of which is induced by the relationship between the auxiliary variable and the original one, and the other is the modified quadratic energy. It should be noted that the new system is equivalent to the original problem only under the consistent initial condition. In fact, the original energy reduces as a weak invariant of the new system [29]. This process is called the QAV reformulation, which provides an elegant platform for developing energy-preserving schemes. Then symplectic RK methods are employed for the QAV reformulated system, which results in the so-called QAVRK methods. We note that the QAVRK schemes could naturally conserve all quadratic invariants of the new system. Under the consistent initial condition, this new class of methods can inherit the relationship between the

auxiliary variable and the original one, and thus can be reduced to an equivalent format by eliminating the auxiliary variable. The proposed methods are proved rigorously to conserve the original energy exactly. Furthermore, the QAVRK methods are symmetric when RK coefficients also satisfy the condition of symmetry. More interesting is that the discrete variational derivative method presented in Ref. [40] is a special case of our proposed methods. It is worth noting that one can directly apply a class of RK methods to develop energy-preserving algorithms without increasing the computational cost compared with the underlying RK methods. In the numerical experiments, we focus on the QAVRK methods with the Gaussian collocation coefficients, which satisfy the symplectic and symmetric conditions. Numerical results are presented to demonstrate the accuracy, conservative property and efficiency of the proposed methods.

The rest of this paper is organized as follows. In Section 2, the QAV approach is proposed to reformulate the CH equation. Then in Section 3, the QAVRK methods are presented, and their properties are discussed. Numerical examples are shown to validate the efficiency and accuracy of our proposed schemes in Section 4. Finally, we give some conclusions in the last section.

2. QAV reformulation. In this section, we present the QAV reformulation for the CH equation. The reformulated system is shown to possess two strong quadratic invariants, which lead to the original energy conservation law under the consistent initial condition. It is worth noting that the QAV reformulation will provide an elegant platform for developing novel arbitrarily high-order structure-preserving algorithms that conserve the original energy exactly.

As we know, Eq. (1.1) can be rewritten equivalently into the following Hamiltonian system

$$u_t = \mathcal{D}\frac{\delta \mathcal{H}}{\delta u}, \tag{2.1}$$

where $\mathcal{D} = -(1-\partial_{xx})^{-1}\partial_x$ is a skew-adjoint operator, $\mathcal{H} = \frac{1}{2}\int_a^b (u^3 + uu_x^2)\mathrm{d}x$ is the Hamiltonian energy, and $\frac{\delta \mathcal{H}}{\delta u}$ denotes the variational derivative of $\mathcal{H}$ with respect to u

$$\frac{\delta \mathcal{H}}{\delta u} = \frac{3}{2}u^2 + \frac{1}{2}u_x^2 - (uu_x)_x. \tag{2.2}$$

Under periodic boundary condition, the model (2.1) satisfies the energy conservation law

$$\frac{\mathrm{d}\mathcal{H}}{\mathrm{d}t} = \left(\frac{\delta \mathcal{H}}{\delta u}, u_t\right) = \left(\frac{\delta \mathcal{H}}{\delta u}, \mathcal{D}\frac{\delta \mathcal{H}}{\delta u}\right) = 0, \tag{2.3}$$

where $(f,g) := \int_a^b f \cdot g\mathrm{d}x$, and the associated L^2 norm $\|f\| = \sqrt{(f,f)}$ for all $f, g \in L^2([a,b])$.

Next we present the QAV approach to reformulate the CH equation. Introducing a quadratic auxiliary variable

$$q = u^2 + u_x^2, \tag{2.4}$$

the original energy can be transformed into a modified quadratic form

$$\mathcal{E} := \mathcal{E}[u,q] = \frac{1}{2}(u,q). \tag{2.5}$$

According to energy variational principle, we reformulate the model (2.1) into an equivalent system

$$\begin{cases} u_t = \mathcal{D}\left(\frac{1}{2}q + u^2 - (uu_x)_x\right), \\ q_t = 2uu_t + 2u_x u_{xt}, \end{cases} \tag{2.6}$$

with the consistent initial condition

$$q(x,0) = u^2(x,0) + u_x^2(x,0). \tag{2.7}$$

THEOREM 2.1. *The QAV system (2.6) possesses two strong quadratic invariants*

$$\mathcal{Q}(x,t) := q - u^2 - u_x^2 \equiv \mathcal{Q}(x,0), \quad \forall\, x,t, \tag{2.8}$$

$$\mathcal{E}(t) := \frac{1}{2}(u,q) \equiv \mathcal{E}(0), \quad \forall\, t. \tag{2.9}$$

Proof. The second equation of the QAV system (2.6) can be written as

$$\partial_t(q - u^2 - u_x^2) = 0,$$

which implies (2.8). By some calculations, we can deduce the modified energy conservation law from the QAV system (2.6)

$$\begin{aligned}
\frac{\mathrm{d}\mathcal{E}}{\mathrm{d}t} &= \frac{1}{2}(u_t,q) + \frac{1}{2}(u,q_t)\\
&= \frac{1}{2}(u_t,q) + (u, uu_t + u_xu_{xt})\\
&= \left(\frac{1}{2}q + u^2 - (uu_x)_x, u_t\right)\\
&= \left(\frac{1}{2}q + u^2 - (uu_x)_x, \mathcal{D}\left(\frac{1}{2}q + u^2 - (uu_x)_x\right)\right)\\
&= 0,
\end{aligned}$$

which leads to (2.9). The proof is complete. ∎

THEOREM 2.2. *Under the consistent initial condition (2.7), the QAV system (2.6) conserves the original energy conservation law*

$$\mathcal{H}(t) = \frac{1}{2}\big(u, u^2 + u_x^2\big) \equiv \mathcal{H}(0), \quad \forall t. \tag{2.10}$$

Proof. Combining the consistent initial condition (2.7) with the conservative property (2.8) leads to the relationship (2.4), which implies that the QAV system (2.6) with (2.7) is equivalent to the original model (2.1) and thus (2.10) holds. This completes the proof. ∎

REMARK 2.1. *Although the existing energy quadratization approaches (IEQ [48] or SAV [43]) can provide a fundamental treatments to solve almost all problems, they are difficult to maintain the original energy structure. Actually, the relationship (2.4) and the original energy conservation law hold for the consistent initial condition (2.7), so they are weak properties of the new system (2.6). As we know, the RK methods satisfying the symplectic condition naturally conserve all quadratic invariants, so they can maintain these weak properties. Therefore, based on our QAV reformulation, one can easily develop numerical methods to preserve the original energy structure, which will be presented in the next section.*

3. QAVRK methods. In this section, we present a new class of QAVRK methods for the CH equation. The proposed schemes are proved to preserve the original energy conservation law if RK coefficients satisfy the symplectic condition. Furthermore, the symmetry of the QAVRK methods is discussed.

Applying an s-stage RK method to the QAV system (2.6), we obtain the following QAVRK scheme.

SCHEME 3.1 (s-stage QAVRK method). *Let a_{ij}, b_i, c_i $(i,j = 1,\cdots,s)$ be a set of RK coefficients.*

For given (u^n, q^n), the following intermediate values are first calculated by

$$\begin{cases} U_i = u^n + \Delta t \sum\limits_{j=1}^{s} a_{ij} k_j, \\ Q_i = q^n + \Delta t \sum\limits_{j=1}^{s} a_{ij} l_j, \\ k_i = \mathcal{D}\left(\frac{1}{2} Q_i + U_i^2 - \partial_x (U_i \partial_x U_i)\right), \\ l_i = 2 U_i k_i + 2 \partial_x U_i \partial_x k_i. \end{cases} \tag{3.1}$$

Then (u^{n+1}, q^{n+1}) is updated via

$$u^{n+1} = u^n + \Delta t \sum_{i=1}^{s} b_i k_i, \tag{3.2}$$

$$q^{n+1} = q^n + \Delta t \sum_{i=1}^{s} b_i l_i. \tag{3.3}$$

Note that **Scheme 3.1** is a time semi-discrete system, where the variables $U_i, Q_i, k_i, l_i, u^{n+1}$ and q^{n+1} are functions of the spatial variable x. As we know, if RK coefficients satisfy

$$b_i a_{ij} + b_j a_{ji} = b_i b_j, \quad \forall\ i, j = 1, \cdots, s, \tag{3.4}$$

the resulting RK method can conserve all strong quadratic invariants [14]. It is well known that (3.4) is also symplectic condition since the corresponding RK method is symplectic-preserving [29]. Therefore, we have the following lemma.

LEMMA 3.1. *Under the consistent initial condition*

$$q^0 = \left(u^0\right)^2 + \left(\partial_x u^0\right)^2,$$

the QAVRK method with the symplectic condition inherits the relationship between the auxiliary variable and the original variable, i.e.,

$$q^n = \left(u^n\right)^2 + \left(\partial_x u^n\right)^2, \quad \forall\ n. \tag{3.5}$$

Proof. According to Eq. (3.2), one can obtain

$$\left(u^{n+1}\right)^2 - \left(u^n\right)^2 = 2\Delta t \sum_{i=1}^{s} b_i k_i u^n + \Delta t^2 \sum_{i,j=1}^{s} b_i b_j k_i k_j. \tag{3.6}$$

Applying $u^n = U_i - \Delta t \sum\limits_{j=1}^{s} a_{ij} k_j$ to the right hand side of (3.6), it yields

$$\left(u^{n+1}\right)^2 - \left(u^n\right)^2 = 2\Delta t \sum_{i=1}^{s} b_i k_i U_i, \tag{3.7}$$

where $\sum_{i,j=1}^{s} b_i a_{ij} k_i k_j = \sum_{i,j=1}^{s} b_j a_{ji} k_i k_j$ and the condition (3.4) were used. Similarly, we have

$$\left(\partial_x u^{n+1}\right)^2 - \left(\partial_x u^n\right)^2 = 2\Delta t \sum_{i=1}^{s} b_i \partial_x k_i \partial_x U_i. \tag{3.8}$$

Adding (3.7) and (3.8), then using (3.1) and (3.3), we can deduce

$$q^{n+1} - \left(u^{n+1}\right)^2 - \left(\partial_x u^{n+1}\right)^2 = q^n - \left(u^n\right)^2 - \left(\partial_x u^n\right)^2, \quad \forall\ n. \tag{3.9}$$

Under the consistent initial condition, we can obtain (3.5) from (3.9), which completes the proof. ∎

When the relationship (3.5) is restored, we can eliminate the auxiliary variable in **Scheme 3.1** and obtain the following QAVRK method for the original CH equation.

SCHEME 3.2 (s-stage QAVRK method). *Let a_{ij}, b_i, c_i $(i,j=1,\cdots,s)$ be a set of RK coefficients. For given u^n, the following intermediate values are first calculated by*

$$\begin{cases} U_i = u^n + \Delta t \sum\limits_{j=1}^{s} a_{ij} k_j, \\ Q_i = \left(u^n\right)^2 + \left(\partial_x u^n\right)^2 + 2\Delta t \sum\limits_{j=1}^{s} a_{ij}(U_j k_j + \partial_x U_j \partial_x k_j), \\ k_i = \mathcal{D}\left(\frac{1}{2} Q_i + U_i^2 - \partial_x\big(U_i \partial_x U_i\big)\right). \end{cases} \tag{3.10}$$

Then u^{n+1} is updated via

$$u^{n+1} = u^n + \Delta t \sum_{i=1}^{s} b_i k_i. \tag{3.11}$$

Different from existing RK methods, **Scheme 3.2** should be regarded as a new class of RK methods for the original CH equation. According to **Lemma 3.1**, **Scheme 3.1** is equivalent to **Scheme 3.2** for a kind of RK methods that satisfy the symplectic condition. Next, we prove the structure-preserving properties of the new methods.

THEOREM 3.1. *All QAVRK methods conserve the linear mass invariant, i.e., $(u^{n+1},1)=(u^n,1)$. If RK coefficients satisfy the symplectic condition (3.4), then the resulting QAVRK method preserves the original energy conservation law*

$$\mathcal{H}^{n+1} = \mathcal{H}^n, \qquad \mathcal{H}^n = \frac{1}{2}\Big(u^n, \left(u^n\right)^2 + \left(\partial_x u^n\right)^2\Big). \tag{3.12}$$

Proof. Noticing that $\mathcal{D} = -(1-\partial_{xx})^{-1}\partial_x$ is skew-adjoint, thus taking the inner product of the last equation of the system (3.10) with the constant function 1, we have

$$(k_i, 1) = -\left(\frac{1}{2} Q_i + U_i^2 - \partial_x\big(U_i \partial_x U_i\big), \mathcal{D}\cdot 1\right) = 0, \tag{3.13}$$

which leads to the mass conservation

$$\big(u^{n+1},1\big) = \big(u^n,1\big) + \Delta t \sum_{i=1}^{s} b_i (k_i,1) = \big(u^n,1\big).$$

Reintroducing the following variables

$$q^n = \left(u^n\right)^2 + \left(\partial_x u^n\right)^2, \quad q^{n+1} = \left(u^{n+1}\right)^2 + \left(\partial_x u^{n+1}\right)^2, \quad l_i = 2U_i k_i + 2\partial_x U_i \partial_x k_i,$$

and Q_i in **Scheme 3.2** can be rewritten as

$$Q_i = q^n + \Delta t \sum_{j=1}^{s} a_{ij} l_j.$$

According to (3.7) and (3.8), we can obtain from **Scheme 3.2** that

$$q^{n+1} = q^n + \Delta t \sum_{i=1}^{s} b_i l_i.$$

Similar to the proof of Eq. (3.7), we have

$$\begin{aligned}
\mathcal{H}^{n+1}-\mathcal{H}^n &= \frac{1}{2}(u^{n+1},q^{n+1})-\frac{1}{2}(u^n,q^n)\\
&= \frac{\Delta t}{2}\sum_{i=1}^{s} b_i\Big((k_i,Q_i)+(U_i,l_i)\Big)\\
&= \frac{\Delta t}{2}\sum_{i=1}^{s} b_i\Big((k_i,Q_i)+(U_i,2U_ik_i+2\partial_xU_i\partial_xk_i)\Big)\\
&= \Delta t\sum_{i=1}^{s} b_i\Big(k_i,\frac{1}{2}Q_i+U_i^2-\partial_x\big(U_i\partial_xU_i\big)\Big)\\
&= \Delta t\sum_{i=1}^{s} b_i\left(\mathcal{D}\left(\frac{1}{2}Q_i+U_i^2-\partial_x\big(U_i\partial_xU_i\big)\right),\frac{1}{2}Q_i+U_i^2-\partial_x\big(U_i\partial_xU_i\big)\right)\\
&= 0.
\end{aligned}$$

The proof is completed. ∎

THEOREM 3.2. *If RK coefficients satisfy the symplectic condition (3.4), then the adjoint method of* ***Scheme 3.2*** *is again an s-stage QAVRK method, whose coefficients are given by*

$$a_{ij}^*=b_{s+1-j}-a_{s+1-i,s+1-j},\quad b_i^*=b_{s+1-i}. \tag{3.14}$$

If RK coefficients satisfy not only the symplectic condition (3.4), but also the following symmetric condition

$$a_{ij}+a_{s+1-i,s+1-j}=b_j,\quad \forall\, i,j, \tag{3.15}$$

then ***Scheme*** *3.2 is symmetric.*

Proof. Exchanging $u^n\leftrightarrow u^{n+1}$ and $\Delta t\leftrightarrow-\Delta t$ in the QAVRK formulas yields

$$\begin{cases}
U_i=u^{n+1}-\Delta t\sum\limits_{j=1}^{s}a_{ij}k_j,\\
Q_i=\big(u^{n+1}\big)^2+\big(\partial_xu^{n+1}\big)^2-2\Delta t\sum\limits_{j=1}^{s}a_{ij}(U_jk_j+\partial_xU_j\partial_xk_j),\\
k_i=\mathcal{D}\left(\frac{1}{2}Q_i+U_i^2-\partial_x\big(U_i\partial_xU_i\big)\right),\\
u^n=u^{n+1}-\Delta t\sum\limits_{i=1}^{s}b_ik_i,
\end{cases} \tag{3.16}$$

which can be written equivalently as

$$\begin{cases}
U_i=u^n+\Delta t\sum\limits_{j=1}^{s}(b_j-a_{ij})k_j,\\
Q_i=\big(u^n\big)^2+\big(\partial_xu^n\big)^2+2\Delta t\sum\limits_{j=1}^{s}(b_j-a_{ij})(U_jk_j+\partial_xU_j\partial_xk_j)\\
\qquad\qquad +\Delta t^2\sum\limits_{i,j=1}^{s}(b_ia_{ij}+b_ja_{ji}-b_ib_j)(k_ik_j+\partial_xk_i\partial_xk_j),\\
k_i=\mathcal{D}\left(\frac{1}{2}Q_i+U_i^2-\partial_x\big(U_i\partial_xU_i\big)\right),\\
u^{n+1}=u^n+\Delta t\sum\limits_{i=1}^{s}b_ik_i.
\end{cases} \tag{3.17}$$

Noticing that the values $\sum_{j=1}^{s}(b_j - a_{ij}) = 1 - c_i$ appear in reverse order, then denoting $k_i^* = k_{s+1-i}$, $U_i^* = U_{s+1-i}$, $Q_i^* = Q_{s+1-i}$ and using (3.4) and (3.14), the adjoint method reads

$$\begin{cases} U_i^* = u^n + \Delta t \sum_{j=1}^{s} a_{ij}^* k_j^*, \\ Q_i^* = \left(u^n\right)^2 + \left(\partial_x u^n\right)^2 + 2\Delta t \sum_{j=1}^{s} a_{ij}^* (U_j^* k_j^* + \partial_x U_j^* \partial_x k_j^*), \\ k_i^* = \mathcal{D}\left(\frac{1}{2} Q_i^* + (U_i^*)^2 - \partial_x\left(U_i^* \partial_x U_i^*\right)\right), \\ u^{n+1} = u^n + \Delta t \sum_{i=1}^{s} b_i^* k_i^*, \end{cases} \tag{3.18}$$

which is a new s-stage QAVRK method. In addition, the assumption (3.15) implies $a_{ij}^* = a_{ij}$ and $b_i^* = b_i$, so that the QAVRK method is symmetric. ∎

REMARK 3.1. *Since the intermediate variables $\{U_i\}$ and $\{Q_i\}$ can be regarded as functions of $\{k_i\}$, the system (3.10) is only a nonlinear system of equations of $\{k_i\}$, whose computational cost is similar to the underlying RK method.*

REMARK 3.2. *Although energy-preserving HBVMs have been proved to be equivalent to a certain RK method [4], it is difficult to construct energy-preserving algorithms using the classical RK methods directly. To our surprise, the QAVRK method presented in this paper provides a new technique that allows a class of RK methods to be directly applied to develop energy-preserving schemes for general conservative systems with polynomial invariants.*

REMARK 3.3. *It is well known that Gauss RK methods satisfy the symplectic condition (3.4), so they can be directly used to develop energy-preserving QAVRK methods. For convenience, the s-stage QAVRK scheme with the Gaussian collocation coefficients is called QAV-GRK-s method. Since the Gaussian collocation coefficients also satisfy the symmetric condition (3.15), thus the QAV-GRK-s method is symmetric. Specially, the QAV-GRK-1 reads*

$$\begin{cases} U = u^n + \frac{\Delta t}{2} k, \\ Q = \left(u^n\right)^2 + \left(\partial_x u^n\right)^2 + \Delta t\left(Uk + \partial_x U \partial_x k\right), \\ k = \mathcal{D}\left(\frac{1}{2} Q + U^2 - \partial_x\left(U \partial_x U\right)\right), \\ u^{n+1} = u^n + \Delta t k. \end{cases} \tag{3.19}$$

Eliminating U, Q, k, one gets

$$\frac{u^{n+1} - u^n}{\Delta t} = \mathcal{D}\left(\frac{(u^{n+1})^2 + u^n u^{n+1} + (u^n)^2}{2} + \frac{(u_x^{n+1})^2 + (u_x^n)^2}{4} - \left(\frac{u^{n+1} + u^n}{2} \frac{u_x^{n+1} + u_x^n}{2}\right)_x\right). \tag{3.20}$$

It is readily to show that the scheme (3.20) can be also obtained by applying the Furihata's method for the original model (2.1) (see [21, 40]). Therefore, for the CH equation, the discrete variational derivative method is a special case of our proposed methods. It is worth pointing out that the Furihata's method is only of order 2, while our QAV-GRK-s method is of order $2s$.

REMARK 3.4. *After appropriate spatial discretization that satisfies the discrete integration-by-parts formula (see [24, 25] for details), the QAVRK method naturally leads to a fully discrete energy-preserving scheme. In this paper, we employ the Fourier pseudo-spectral method for spatial discretization. We omit the details here due to save space. Interested readers are referred to our earlier work [24, 31] for details.*

4. Numerical results. In this section, we provide some numerical results to illustrate the accuracy and robustness of the energy-preserving QAV-GRK-s scheme. Both spatial and temporal convergence rates are shown via a smooth solution. We then use the wave propagation as a benchmark to demonstrate

that the proposed algorithm produces physical accurate results and the property of energy conservation. We also present some numerical comparisons with linear-implicit Crank-Nicolson momentum-preserving scheme [31] (abbr. LCN-MP), linear-implicit Crank-Nicolson energy-preserving scheme based on energy quadratization technique (abbr. LCN-EP), AVF method and HBVMs. These simulations are performed by using the Newton iteration method in which the nonlinear iterative tolerance is set as $\mathrm{Tol} = 1.0\times10^{-14}$ and the number of maximum iterative step is fixed to $M = 100$ in most cases, and it may changes for some specific cases, which we mention, as appropriate.

4.1. Accuracy test.

EXAMPLE 1 (Convergence rates). *To begin with, we present an example of smooth traveling waves to demonstrate the convergences of the proposed schemes herein against both the spatial and temporal step size. According to [37], we introduce four parameters $c, m, M, z \in \mathbb{R}$ with $z = c - M - m$ to describe the traveling waves. If $z < m < M < c$, then there exists a smooth periodic traveling wave solution for $x \in [0, L]$*

$$u(x,t) = \phi(x - ct) = \begin{cases} \phi(x-l), & x \in [l, L], \\ \phi(x-l+L), & x \in [0, l], \end{cases} \tag{4.1}$$

where $l = \mathrm{mod}(ct, L)$. And $\phi(x)$ satisfy the following parametric equations

$$\begin{cases} \phi = m + (M-m)\sin^2\theta, \\ x = 2\displaystyle\int_0^\theta \frac{\sqrt{A-\sin^2 t}}{\sqrt{B+\sin^2 t}}\mathrm{d}t, \end{cases} \tag{4.2}$$

with $\theta \in [0, \pi]$, $A = \frac{c-m}{M-m}$ and $B = \frac{m-z}{M-m}$. In this test, we choose parameters $m = 0.3$, $M = 0.8$ and $c = 1.3$. This means the wave has period $L \approx 10.766837967585580$, which can be numerically calculated by

$$L = 2\int_0^\pi \frac{\sqrt{A-\sin^2 t}}{\sqrt{B+\sin^2 t}}\mathrm{d}t. \tag{4.3}$$

In the spatial test, we take QAV-GRK-2 as a representative to test the spatial accuracy in which the time step is set as $\tau = 10^{-4}$ to prevent errors in time discretization from contaminating our results. We vary the number of Fourier nodes systematically between 8 and 64. The discrete L^2 and L^∞ errors at $t = 1$ are recorded in Figure 4.1, which clearly exhibits an exponential convergence rate.

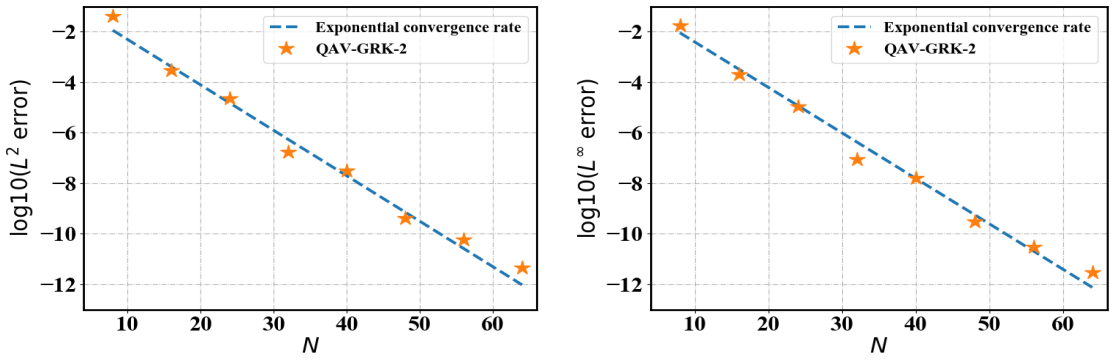

FIG. 4.1. **Example 1:** *Spatial convergence test for the QAV-GRK-2 scheme. These figures indicate that such a convergence behavior is often said to have spectral accuracy in space.*

For the time accuracy test, if we instead keep $N = 128$ fixed by using Fourier pseudo-spectral method in space, and decrease the time step, the convergence orders that calculated by some structure-preserving numerical schemes (i.e., LCN-EP, LCN-MP, AVF, HBVM(3,2), HBVM(5,3), QAV-GRK-2, and QAV-GRK-3) at the final time $t = 1$ are displayed in Figure 4.2. It can be observed that the proposed numerical methods exhibit the expected convergence rate in time. Obviously, the errors of the QAV-GRK-3 scheme are significantly smaller than those of QAV-GRK-2 with the same time step. In particular, both the high-order QAV-GRK schemes are also significantly smaller than the second-order scheme in several orders of magnitude and perform slightly better than HBVMs. In a word, the above numerical behaviors highlight the advantage of the newly proposed QAVRK schemes.

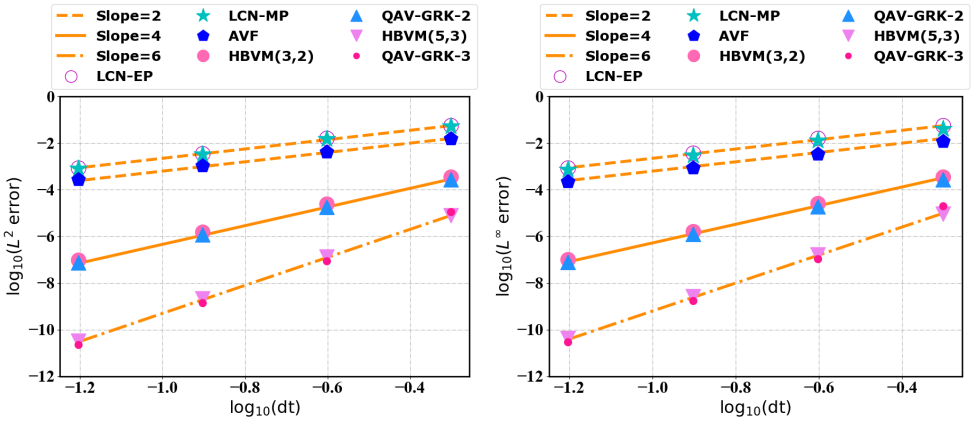

FIG. 4.2. **Example 1:** *Temporal mesh refinement test for various numerical schemes. Here both the L^2 and L^∞ errors using different time steps are shown. One can clearly observe that the two high-order QAVRK schemes provide their expected high-order temporal accuracy. Moreover, the numerical errors of the high-order QAVRK schemes are much smaller than that of the second-order schemes and perform slightly better than other high-order HBVMs.*

To further illustrate the merits of the high-order QAV-GRK schemes, we test the L^∞ errors of numerical solution at $t = 1$ smaller than 10^{-10} in which the approximate time steps are $\tau = 10^{-5}$ for the second-order schemes, (i.e., LCN-EP, LCN-MP, AVF), $\tau = 0.004$ for HBVM(3,2) and the QAV-GRK-2 scheme, and $\tau = 0.02$ for HBVM(5,3) and the QAV-GRK-3 scheme. The total CPU time is tabulated in Table 4.1. It illustrates the high-order QAVRK schemes take less CPU time than the lower ones and HBVMs to the expected accuracy. This indicates our newly developed high-order QAVRK schemes are superior to other numerical methods for accurate long-time dynamic simulations.

TABLE 4.1
Total CPU time using various numerical schemes solving the CH equation.

Scheme	time-step τ	CPU time
AVF	1×10^{-5}	2842.87
LCN-MP	1×10^{-5}	53.81
LCN-EP	1×10^{-5}	51.78
HBVM(3,2)	4×10^{-3}	1.85
QAV-GRK-2	4×10^{-3}	1.69
HBVM(5,3)	2×10^{-2}	2.43
QAV-GRK-3	2×10^{-2}	0.93

In addition to solving nonlinear system using the Newton iteration method, we also deal with it by

using the fixed-point iteration method and conduct some numerical comparisons. Figure 4.3 depicts the number of Newton iteration and fixed-point iteration in the evolution process with different time steps. It can be observed that time step has a great influence on the number of fixed-point iterations, and at some moments it does not converge even when it reaches our predetermined maximum iteration step. In contrast, the Newton iteration method is predictably stable.

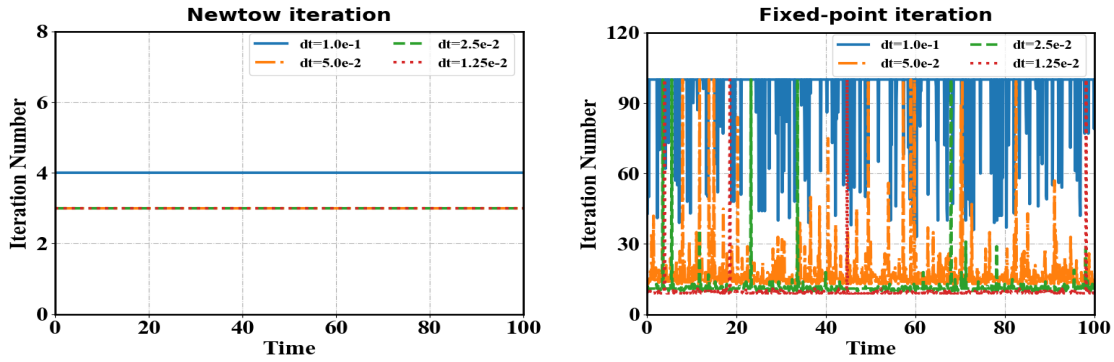

FIG. 4.3. **Example 1:** *Comparisons between the number of Newton iteration and fixed-point iteration in each time step by using the QAV-GRK-2 scheme.*

Finally, based on the above numerical performances, we pick the time step $\Delta t = 0.1$ *for a long-term numerical simulation to examine the changes of the discrete mass, energy and momentum for CH equation. It should be emphasized that we adopt the EIP technique proposed in [22] to prevent the growth of the energy errors in a long time calculation. In Figure 4.4, we present the evolution of the relative error in mass, momentum and energy. From Figure 4.4 (a) and (c), one can see that the original mass and energy are conserved with machine precision by the high-order QAV-GRK schemes. Although the newly developed high-order QAV-GRK schemes can not accurately warrant the momentum conservation, Figure 4.4 (b) supports such a statement that the higher the accuracy of the scheme, the smaller the error of momentum.*

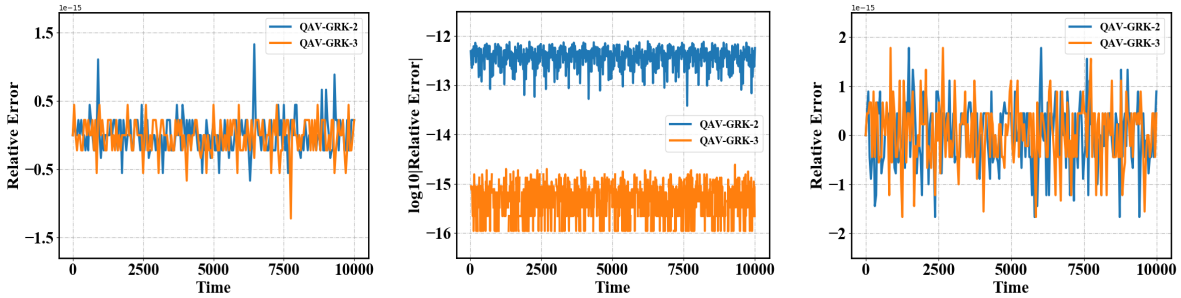

(a) Mass (b) Momentum (c) Energy

FIG. 4.4. **Example 1:** *Time evolutions of the mass, momentum and energy versus time calculated by using our proposed high-order QAV-GRK schemes. Both methods use* $\tau = 0.1$ *and* $N = 128$.

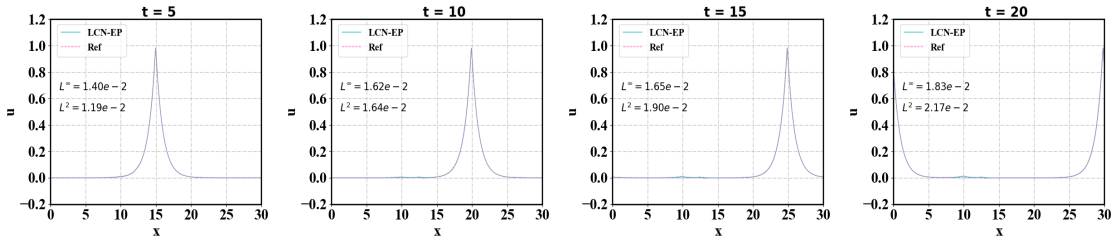

(a) The detail comparison results for the solution of LCN-EP and reference solution with $\tau = 0.005$.

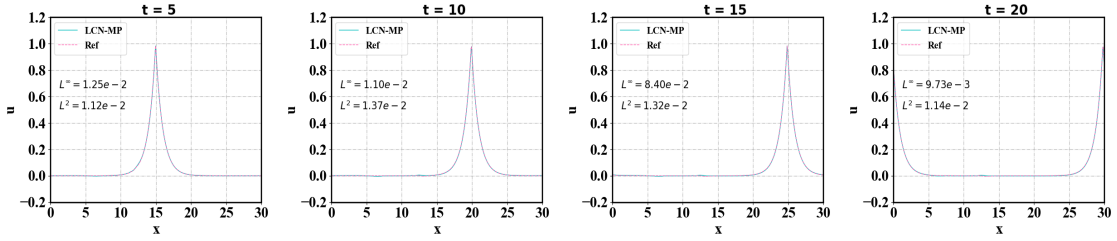

(b) The detail comparison results for the solution of LCN-MP and reference solution with $\tau = 0.005$.

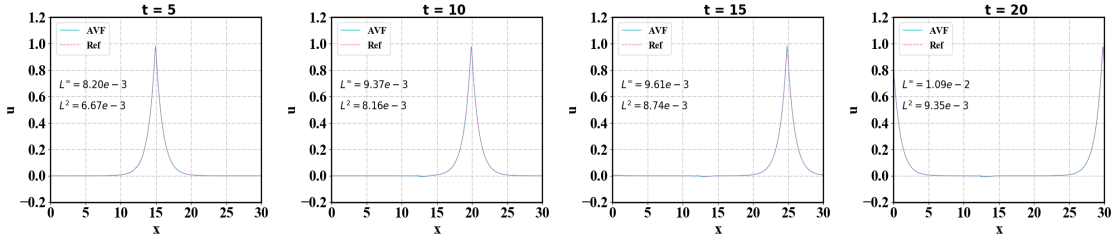

(c) The detail comparison results for the solution of AVF and reference solution with $\tau = 0.01$.

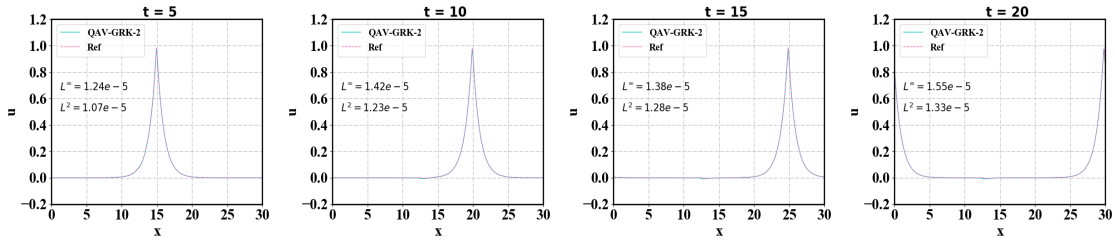

(d) The detail comparison results for the solution of QAV-GRK-2 and reference solution with $\tau = 0.01$.

FIG. 4.5. **Example 2:** *The peakon profiles of the CH equation with the initial condition (4.5) and different numerical schemes. These figures present the profiles of u at time $t = 5, 10, 15, 20$, respectively. It illustrates our proposed schemes are very efficient to deal with the single peakon solution with fairly large time step.*

4.2. Peakon solution. In the next benchmark examples, we consider the periodic traveling wave to test our proposed structure-preserving schemes in which the initial data will be generated from the following profiles:

$$\phi_i(x) = \begin{cases} \frac{c_i}{\cosh(a/2)} \cosh(x - x_i), & |x - x_i| \le \frac{a}{2}, \\ \frac{c_i}{\cosh(a/2)} \cosh(a - (x - x_i)), & |x - x_i| > \frac{a}{2}, \end{cases} \tag{4.4}$$

where c_i, x_i and a to be further determined later.

EXAMPLE 2 (Peakon solution). *In this example, we present the wave propagation of a single peak solution. The initial condition is*

$$u_0(x) = \phi_0(x). \tag{4.5}$$

The parameters are chosen as $a = 30$, $c = 1$ *and* $x_0 = -5$. *We use domain* $\Omega = [0, a]$. *The lack of smoothness at the peak of peakons produces high-frequency dispersive errors in the calculation. To resolve it, we adopt the spatial mesh* $N = 512$ *to maintain the resolution.*

In this study, we only select the second-order schemes as the object of comparison. Since the exact solution is not known, we pick the solution obtained with time step $\tau = 10^{-4}$ *and Tol* $= 1.0\times10^{-8}$ *computed by the sixth-order HBVM(5,3) scheme as the benchmark solution (approximately the exact solution) for computing errors at each instant. The peak profiles with various numerical schemes at* $t = 5, 10, 15, 20$ *are shown in Figure 4.5. In our numerical implementation, we cannot get accurate numerical results for time step size* $\tau > 0.005$ *for the LCN-EP and LCN-MP schemes. But Figure 4.5 (c) shows that the AVF scheme gets relatively good approximate solution for the peakon solution when the time step* $\tau = 0.01$. *However, it follows from Figure 4.5 (d) that, for the high-order QAV-GRK-2 scheme, its accuracy becomes quite satisfactory and it is more accurate than the 2nd AVF scheme under the same conditions.*

We run a long time numerical simulation till $t = 500$ *and plot the relative errors of mass, momentum and the original energy that computed by using QAV-GRK-2 with time step* $\tau = 0.01$ *in Figure 4.6. It indicates that our proposed scheme preserves the original energy conservation and mass very accurately. This is consistent with Theorem 3.1. These numerical behaviors strongly support our claim that the high-order QAV schemes are very efficient to deal with a single peakon interaction very well.*

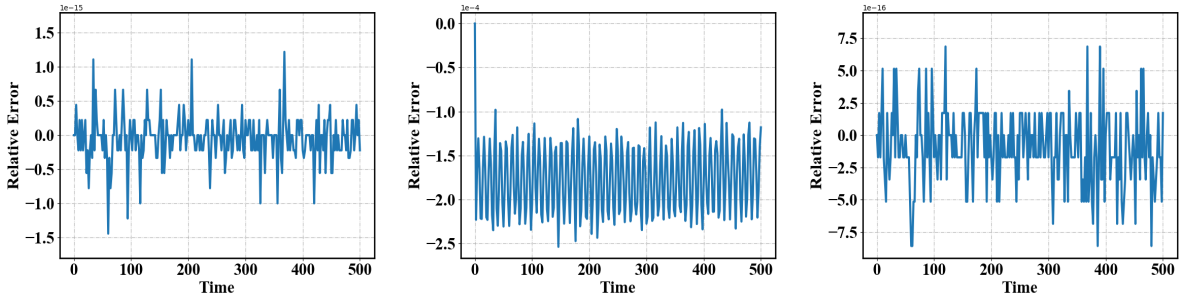

(a) Mass (b) Momentum (c) Energy

FIG. 4.6. **Example 2:** *Long time changes of mass, momentum and energy versus time that computed by using our proposed high-order QAV-GRK-2 scheme with* $\tau = 0.01$. *These curves show our schemes obey the mass and original energy conservation laws.*

EXAMPLE 3 (Two-peakon interaction). *In this test, we study the two peakon interaction of the CH model with the following initial condition*

$$u_0(x) = \sum_{i=1}^{2} \phi_i, \tag{4.6}$$

where ϕ_i *is give by (4.4). The parameters are picked as* $c_1 = 2$, $c_2 = 1$, $x_1 = -5$, $x_2 = 5$. *We choose the domain as* $\Omega = [0, a]$ *and spatial meshes* $N = 512$ *are used to resolve the peakon.*

Here, we choose QAV-GRK-2 and QAV-GRK-3 to simulate two-peakon interaction with the uniform time step $\tau = 0.01$. *Similar to the previous example, the reference solution is obtained by the 6th*

HBVM(5,3) scheme with time step $\tau = 10^{-4}$ *and* $Tol = 1.0\times10^{-8}$. *The numerical results are summarized in Figure 4.7. One can clearly observe that the moving peakon interaction is resolved very well, where the accuracy of 6th QAV-GRK-3 scheme is obviously higher than the 4th QAV-GRK-2 scheme. These numerical behaviors are consistent with the reported literatures [31, 39, 47].*

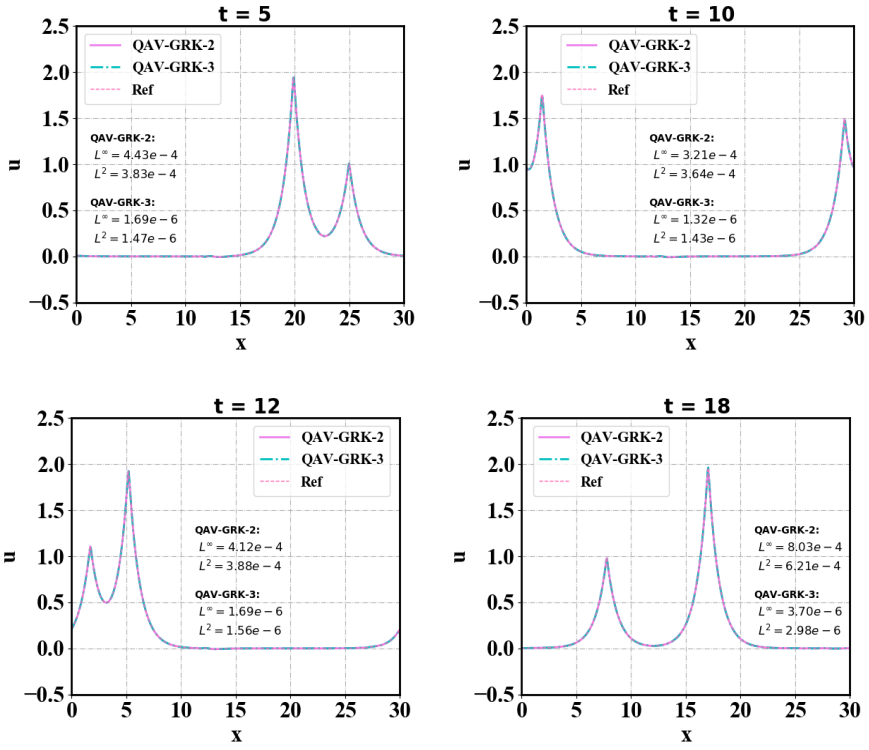

FIG. 4.7. **Example 3:** *Evolutions of two-peakon interaction in terms of* u *with time step* $\tau = 0.01$. *Snapshots are taken at* $t = 5, 10, 12, 18$, *respectively. It indicates the high-order QAV-GRK schemes can capture the two-peakon interaction accurately with fairly large time step.*

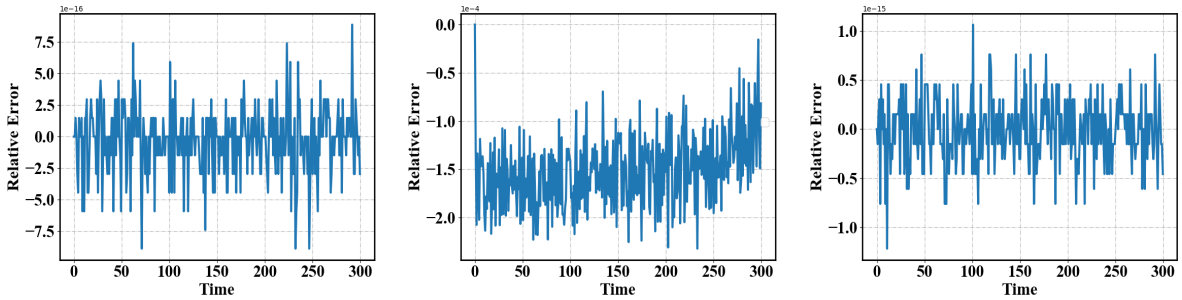

(a) Mass (b) Momentum (c) Energy

FIG. 4.8. **Example 3:** *Evolutions of the relative mass, momentum and energy errors using the QAV-GRK-2 scheme with* $\tau = 0.01$. *The curves of the relative mass and energy errors show our proposed scheme warrants the mass and original energy conservation laws.*

The changes in relative mass, momentum and the original energy are also depicted in Figure 4.8, which is agreeable with energy conservation law (3.12). In a word, these numerical results again illustrate that our newly developed high-order schemes can be applied to predict the wave propagation of two-peak solution accurately.

EXAMPLE 4 (Three-peakon interaction). *In this example, we consider the three peakon interaction of this model and the initial condition is given by*

$$u_0(x) = \sum_{i=1}^{3} \phi_i(x), \tag{4.7}$$

where ϕ_i is defined in (4.4). We fix the parameters $c_1 = 2$, $c_2 = 1$, $c_3 = 0.8$, $x_1 = -5$, $x_2 = -3$, $x_3 = -1$. We consider the domain $\Omega = [0, a]$ with $a = 30$.

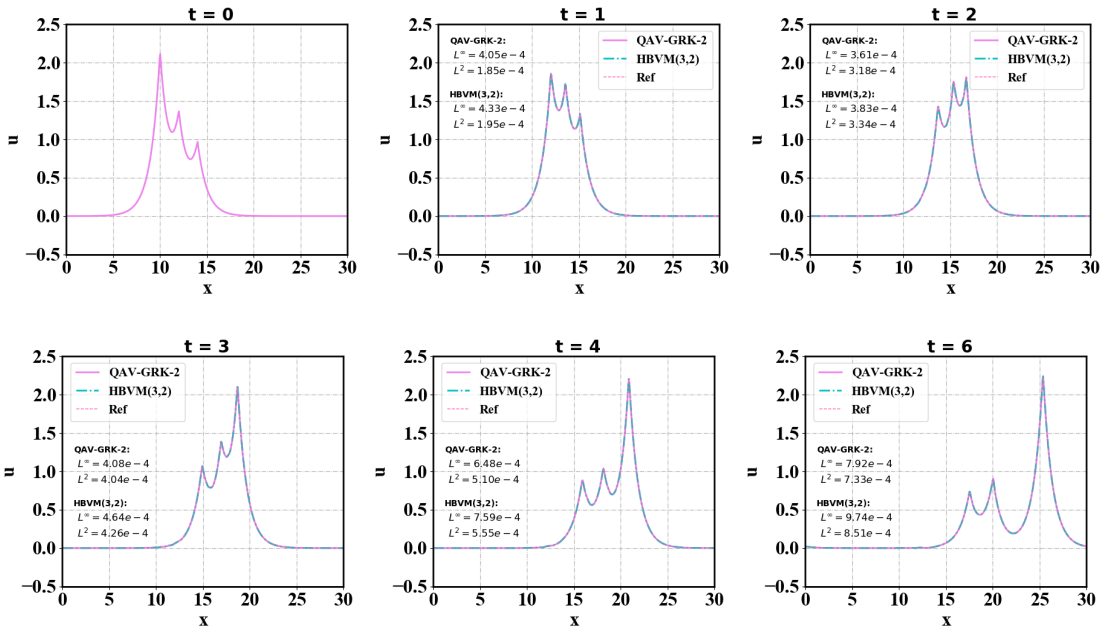

FIG. 4.9. **Example 4:** *Snapshots of three-peakon interaction of the CH equation at time $t = 0, 1, 2, 3, 4, 6$ with the same time step $\tau = 0.01$. It indicates our proposed scheme can accurately predict the three-peakon interaction with fairly large time step.*

To measure the accuracy of the new proposed high-order schemes along with large time step size, we take a uniform time step $\tau = 0.01$ and compare with HBVM. Just as before, we take the numerical solution that calculated by HBVM(5,3) with $\tau = 10^{-4}$ and $Tol = 1.0 \times 10^{-8}$ as a reference at each moment. The numerical results of three-peakon interaction for the CH equation are displayed in Figure 4.9. It is clear that the curves of our scheme and HBVM fit very well with the reference solution. The numerical behaviors agree qualitatively well with those in published literatures, for instance [39, 47]. Meanwhile, we also compute the discrete L^∞ and L^2 errors in every time frame of Figure 4.9, so that we are able to visualize the difference according to the errors. One can observe the QAV-GRK-2 scheme is a little better than HBVM in predicting three-peakon interaction with relatively large time step.

Finally, we present the time evolution of the relative mass, momentum and the original energy in Figure 4.10. The curves of the relative mass and original energy errors are up to machine epsilon, which

confirms the theoretical results that our newly devised high-order QAV schemes can warrant the original energy conservation.

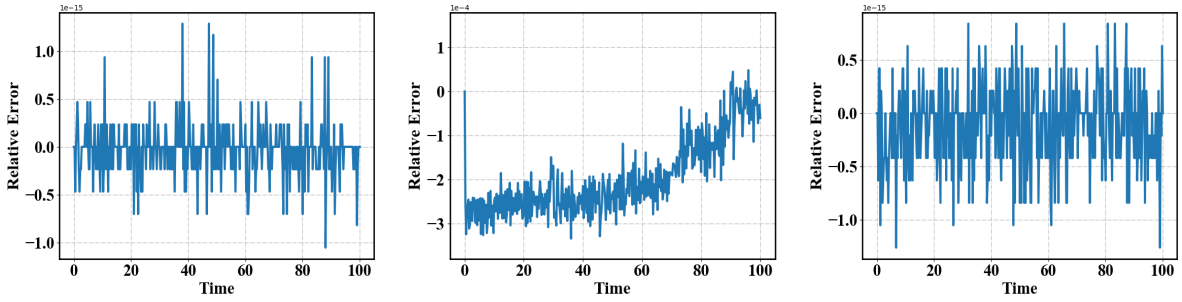

(a) Mass (b) Momentum (c) Energy

FIG. 4.10. **Example 4:** *Time evolutions of the mass, momentum and energy versus time that computed by using our proposed high-order QAV-GRK-2 scheme with* $\tau = 0.01$*. It indicates our developed scheme presents a better conservation of the mass and original energy.*

5. Conclusion. In this paper, we present a new general framework for developing high-order energy-preserving algorithms, which we call the QAVRK schemes. The key of the QAVRK method is the QAV reformulation, which makes the original energy conservation law equivalent to two quadratic invariants of the reformulated model. Since the symplectic RK methods can conserve all quadratic invariants, they can be directly applied for the QAV reformulated system to arrive at energy-preserving methods for the original model. Different from the energy quadratization approaches (IEQ or SAV), the QAVRK method can directly eliminate the auxiliary variable and retain the original energy conservation law. The QAVRK methods are illustrated by the Camassa-Holm equation. Some numerical tests are shown to demonstrate the accuracy, conservative property and efficiency of the proposed schemes. It is worthwhile to emphasize that the presented numerical strategy in this paper can be generalized for conservative systems with non-polynomial invariant, which will be further studied in our future work.

Acknowledgment. Yuezheng Gong's work is partially supported by the Foundation of Jiangsu Key Laboratory for Numerical Simulation of Large Scale Complex Systems (Grant No. 202002), the Natural Science Foundation of Jiangsu Province (Grant No. BK20180413) and the National Natural Science Foundation of China (Grants No. 11801269, 12071216). Qi Hong's work is partially supported by the China Postdoctoral Science Foundation (Grant No. 2020M670116), the Foundation of Jiangsu Key Laboratory for Numerical Simulation of Large Scale Complex Systems (Grant No. 202001). Chunwu Wang's work is partially supported by Science Challenge Project (Grant No. TZ2018002). Yushun Wang's work is partially supported by the National Key Research and Development Program of China (Grant No. 2018YFC1504205) and the National Natural Science Foundation of China (Grants No. 11771213, 61872422, 11971242).

REFERENCES

[1] G. Akrivis, B. Li, and D. Li. Energy-decaying extrapolated RK-SAV methods for the Allen-Cahn and Cahn-Hilliard equations. *SIAM Journal on Scientific Computing*, 41(6):A3703–A3727, 2019.

[2] R. Artebrant and H. Schroll. Numerical simulation of Camassa-Holm peakons by adaptive upwinding. *Applied Numerical Mathematics*, 56:695–711, 2006.

[3] L. Brugnano, M. Calvo, J.I. Montijano, and L. Randez. Energy-preserving methods for Poisson systems. *Journal of Computational and Applied Mathematics*, 236(16):3890–3904, 2012.

[4] L. Brugnano, F. Iavernaro, and D. Trigiante. Hamiltonian boundary value methods (energy preserving discrete line integral methods). *Journal of Numerical Analysis, Industrial and Applied Mathematics*, 5(1-2):17–37, 2010.

[5] L. Brugnano, F. Iavernaro, and R. Zhang. Arbitrarily high-order energy-preserving methods for simulating the gyro-center dynamics of charged particles. *Journal of Computational and Applied Mathematics*, 380:112994, 2020.

[6] W. Cai, Y. Sun, and Y. Wang. Geometric numerical integration for peakon b-family equations. *Communications in Computational Physics*, 19(1):24–52, 2016.

[7] M. Calvo, A. Iserles, and A. Zanna. Numerical solution of isospectral flows. *Mathematics of Computation*, 66(220):1461–1486, 1997.

[8] R. Camassa and D. Holm. An integrable shallow water equation with peaked solitons. *Physical Review Letters*, 71(11):1661–1664, 1993.

[9] G. Coclite, K. Karlsen, and N. Risebro. A convergent finite difference scheme for the Camassa-Holm equation with general H^1 initial data. *SIAM Journal on Numerical Analysis*, 46(3):1554–1579, 2008.

[10] D. Cohen and E. Hairer. Linear energy-preserving integrators for Poisson systems. *BIT*, 51(1):91–101, 2011.

[11] D. Cohen, B. Owren, and X. Raynaud. Multi-symplectic integration of the Camassa-Holm equation. *Journal of Computational Physics*, 227:5492–5512, 2008.

[12] D. Cohen and X. Raynaud. Geometric finite difference schemes for the generalized hyperelastic-rod wave equation. *Journal of Computational and Applied Mathematics*, 235:1925–1940, 2011.

[13] A. Constantin. On the scattering problem for the Camassa-Holm equation. *Proceedings of the Royal Society A: Mathematical, Physical and Engineering Sciences*, 457:953–970, 2001.

[14] G.J. Cooper. Stability of Runge-Kutta methods for trajectory problems. *IMA Journal of Numerical Analysis*, 7:1–13, 1987.

[15] M. Dahlby and B. Owren. A general framework for deriving integral preserving numerical methods for PDEs. *SIAM Journal on Scientific Computing*, 33(5):2318–2340, 2011.

[16] H.-H. Dai. Model equations for nonlinear dispersive waves in a compressible Mooney-Rivlin rod. *Acta Mechanica*, 127:193–207, 1998.

[17] S. Eidnes, L. Li, and S. Sato. Linearly implicit structure-preserving schemes for Hamiltonian systems. *Journal of Computational and Applied Mathematics*, 387:112489, 2021.

[18] B. Feng, K. Maruno, and Y. Ohta. A self-adaptive moving mesh method for the Camassa-Holm equation. *Journal of Computational and Applied Mathematics*, 235:229–243, 2010.

[19] M. Fisher and J. Schiff. The Camassa-Holm equation: Conserved quantities and the initial value problem. *Physics Letters A*, 259:371–376, 1999.

[20] B. Fuchssteiner and A.S. Fokas. Symplectic structures, their Bäcklund transformations and hereditary symmetries. *Physica D: Nonlinear Phenomena*, 4(1):47–66, 1981.

[21] D. Furihata. Finite difference schemes for $\frac{\partial u}{\partial t} = (\frac{\partial}{\partial x})^\alpha \frac{\delta G}{\delta u}$ that inherit energy conservation or dissipation property. *Journal of Computational Physics*, 156:181–205, 1999.

[22] Y. Gong, Y. Chen, C. Wang, and Q. Hong. A new class of high-order energy-preserving schemes for the Korteweg-de Vries equation based on the quadritic auxililiary variable (QAV) approach. *Under review*, 2021.

[23] Y. Gong and Y. Wang. An energy-preserving wavelet collocation method for general multi-symplectic formulations of Hamiltonian PDEs. *Communications in Computational Physics*, 20(5):1313–1339, 2016.

[24] Y. Gong, J. Zhao, and Q. Wang. Linear second order in time energy stable schemes for hydrodynamic models of binary mixtures based on a spatially pseudospectral approximation. *Advances in Computational Mathematics*, 44:1573–1600, 2018.

[25] Y. Gong, J. Zhao, and Q. Wang. Second order fully discrete energy stable methods on staggered grids for hydrodynamic phase field models of binary viscous fluids. *SIAM Journal on Scientific Computing*, 40(2):B528–B553, 2018.

[26] Y. Gong, J. Zhao, and Q. Wang. Arbitrarily high-order linear energy stable schemes for gradient flow models. *Journal of Computational Physics*, 419:109610, 2020.

[27] Y. Gong, J. Zhao, and Q. Wang. Arbitrarily high-order unconditionally energy stable schemes for thermodynamically consistent gradient flow models. *SIAM Journal on Scientific Computing*, 42(1):B135–B156, 2020.

[28] E. Hairer. Energy-preserving variant of collocation methods. *Journal of Numerical Analysis, Industrial and Applied Mathematics*, 5:73–84, 2010.

[29] E. Hairer, C. Lubich, and G. Wanner. *Geometric numerical integration: Structure-preserving algorithms for ordinary differential equations*. Springer-Verlag, Berlin, 2006.

[30] H. Holden and X. Raynaud. Convergence of a finite difference scheme for the Camassa-Holm equation. *SIAM Journal on Numerical Analysis*, 44(4):1655–1680, 2006.

[31] Q. Hong, Y. Gong, and Z. Lv. Linear and Hamiltonian-conserving fourier pseudo-spectral schemes for the Camassa-Holm equation. *Applied Mathematics and Computation*, 346:86–95, 2019.

[32] C. Jiang, W. Cai, and Y. Wang. A linearly implicit and local energy-preserving scheme for the Sine-Gordon equation based on the invariant energy quadratization approach. *Journal of Scientific Computing*, 80:1629–1655, 2019.

[33] C. Jiang, Y. Wang, and Y. Gong. Arbitrarily high-order energy-preserving schemes for the Camassa-Holm equation. *Applied Numerical Mathematics*, 151:85–97, 2020.

[34] C. Jiang, Y. Wang, and Y. Gong. Explicit high-order energy-preserving methods for general Hamiltonian partial differential equations. 388:113298, 2021.

[35] H. Kalisch and J. Lenells. Numerical study of traveling-wave solutions for the Camassa-Holm equation. *Chaos, Solitons and Fractals*, 25:287–298, 2005.

[36] H. Kalisch and X. Raynaud. Convergence of a spectral projection of the Camassa-Holm equation. *Numerical Methods for Partial Differential Equations*, 22:1197–1215, 2006.
[37] J. Lenells. Traveling wave solutions of the Camassa-Holm equation. *Journal of Differential Equations*, 217:393–430, 2005.
[38] H. Li, Y. Wang, and M. Qin. A sixth order averaged vector field method. *Journal of Computational Mathematics*, (5):479–498, 2016.
[39] H. Liu and Y. Xing. An invariant preserving discontinuous Galerkin method for the Camassa-Holm equation. *SIAM Journal on Scientific Computing*, 38(4):A1919–A1934, 2016.
[40] T. Matsuo and H. Yamaguchi. An energy-conserving Galerkin scheme for a class of nonlinear dispersive equations. *Journal of Computational Physics*, 228:4346–4358, 2009.
[41] Y. Miyatake and T. Matsuo. Energy-preserving H^1-Galerkin schemes for shallow water wave equations with peakon solution. *Physics Letters A*, 376:2633–2639, 2012.
[42] G.R.W. Quispel and D.I. Mclaren. A new class of energy-preserving numerical integration methods. *Journal of Physics A Mathematical and Theoretical*, 41:045206, 2008.
[43] J. Shen, J. Xu, and J. Yang. The scalar auxiliary variable (SAV) approach for gradient flows. *Journal of Computational Physics*, 353(15):407–416, 2018.
[44] T. Sheu, P. Chiu, and C. Yu. On the development of a high-order compact scheme for exhibiting the switching and dissipative solution natures in the Camassa-Holm equation. *Journal of Computational Physics*, 230:5399–5416, 2011.
[45] W. Tang and Y. Sun. Time finite element methods: A unified framework for numerical discretizations of ODEs. *Applied Mathematics and Computation*, 219:2158–2179, 2012.
[46] B. Wang and X. Wu. A new high precision energy-preserving integrator for system of oscillatory second-order differential equations. *Physics Letters A*, 376(14):1185–1190, 2012.
[47] Y. Xu and C.-W. Shu. A local discontinuous Galerkin method for the Camassa-Holm equation. *SIAM Journal on Numerical Analysis*, 46(4):1998–2021, 2008.
[48] X. Yang, J. Zhao, and Q. Wang. Numerical approximations for the molecular beam epitaxial growth model based on the invariant energy quadratization method. *Journal of Computational Physics*, 333:104–127, 2017.
[49] H. Zhang, X. Qian, and S. Song. Novel high-order energy-preserving diagonally implicit Runge-Kutta schemes for nonlinear Hamiltonian ODEs. *Applied Mathematics Letters*, 102:106091, 2020.
[50] H. Zhu, S. Song, and Y. Tang. Multi-symplectic wavelet collocation method for the nonlinear Schrödinger equation and the Camassa-Holm equation. *Computer Physics Communications*, 182:616–627, 2011.